

# **Testing an Acoustic Zooplankton Fish Profiler Mounted on a Glider**

A Spatial Temporal Acoustic Survey of Trinity Bay

Kassandra Richard

Supervisor: Len Zedel

Glider Technician: Nicolai von Oppeln-Bronikowski

A thesis presented for the degree of  
Honours in Ocean Physics



Physics and Physical Oceanography  
Memorial University of Newfoundland  
April 7th, 2023

# Contents

<b>List of Figures</b>	<b>II</b>
<b>Abstract</b>	<b>1</b>
<b>1 Introduction</b>	<b>2</b>
1.1 Echosounder Operation when Attached to a Glider . . . . .	2
1.2 Glider Deployment and Sensors . . . . .	4
1.3 Water Properties of Trinity Bay . . . . .	4
<b>2 Theoretical Background</b>	<b>6</b>
2.1 Newton’s Second Law for Acoustics . . . . .	6
2.2 Attenuation and Viscosity . . . . .	9
2.3 Molecular Relaxation . . . . .	11
2.4 Volume Back-scatter Coefficient and Target Strength . . . . .	14
<b>3 Processing</b>	<b>16</b>
<b>4 Results</b>	<b>19</b>
4.1 Back-scatter Diagrams with Different Frequencies . . . . .	19
4.2 Merging Multiple Glider Casts . . . . .	21
4.3 Interpreting Repeated Acoustic Signal . . . . .	24
<b>5 Discussion and Summary</b>	<b>25</b>
<b>References</b>	<b>27</b>

## List of Figures

Figure 1:	Concept of echosounding from page 71 of (Simmonds & MacLennan, 2005). The transmitted pulse generates echos from a fish school and the sea-floor. . . . .	3
Figure 2:	The glider is constrained to travel in up-casts and down-casts on straight, diagonal lines. In this configuration, only back-scatter data collected on down-casts is usable. There are disconnects at the surface because the glider does not collect data there. . . . .	4
Figure 3:	"Barnacle's" Journey in Trinity Bay, November 20th to 30th. Throughout these 10 days, the glider collected 1 054 001 elements with the CTD probes and collected a couple hundred AZFP profiles. . . . .	5
Figure 4:	Acoustic pressure differential across a small volume of fluid from page 36 of (Medwin & Clay, 1998). The pressure differential causes the mass $\Delta x \Delta y \Delta z \rho_a$ to move to the right. . . . .	7
Figure 5:	Sound pressure attenuation rate in dB/km in fresh and seawater from page 109 of (Medwin & Clay, 1998). Calculated from Francios and Garrison (1982). Parameters at pH=8; S=35ppt; and depth z=0 m. . . . .	14
Figure 6:	Pitch of the glider throughout the entire deployment. . . . .	16
Figure 7:	A down-cast associated with an AZFP echo-burst in terms of cumulative distance of the deployment. The average (S,T,P) values from this down-cast are input into Echotype to account for exponential attenuation of the sound-wave during processing. . . . .	17
Figure 8:	Diagram of netcdf file format from ( <i>Lesson 1. Introduction to the NetCDF4 Hierarchical Data Format</i> , 2020) showing that all metadata required to work with the data is in a hierarchical flow. . . . .	18
Figure 9:	Echo diagram of a down-cast, 455 kHz . . . . .	19
Figure 10:	Echo diagram of a down-cast, 200 kHz . . . . .	20
Figure 11:	Echo diagram of a down-cast, 120 kHz . . . . .	20
Figure 12:	Echo diagram of a down-cast, 67 kHz . . . . .	21
Figure 13:	Three AZFP collections stitched together. Frequency channel is 120 kHz. The subtle disconnect on the second down-cast is the beginning of a new AZFP collection. . . . .	22
Figure 14:	A combination of three AZFP collections stitched together. The frequency channel was 120 kHz. The Ultimate goal is to visualize a large portion of Trinity Bay. . . . .	22

Figure 15: The Temperature Profile of Trinity Bay generated from the raw data of the CTD probes from the entire deployment. . . . . 23

Figure 16: The Salinity profile of Trinity Bay generated from the from the CTD data of the entire deployment. . . . . 24

## Abstract

Gliders are autonomous underwater vehicles (AUVs) of approximately 2 m in length that are capable of long-term deployments on the scale of months. They move vertically through the water by altering their buoyancy. The glider's wings convert the vertical force provided by its variable buoyancy device into forward motion, allowing them to also move in a horizontal fashion. Gliders have to operate with limited power-supplies, and therefore cannot replace conventional oceanographic survey cruises. Nevertheless, as more instrumentation options are adapted for gliders, they are rapidly contributing to important oceanographic observations at a fraction of the cost of regular surveys. An example of a low power instrument that can be used on a glider is the Acoustic Zooplankton Fish Profiler (AZFP), which is a multi-frequency echosounder that is used to detect marine species of various sizes. Its original purpose was to be attached to a stationary structure such as a mooring, but recently, the AZFP is being used to augment traditional vessel-based sampling by being attached to gliders. Integrated into gliders, AZFPs can collect data at greater depths, closer to the coast-line, and over longer time periods than vessel-based sampling. This report describes a glider deployment intended to test Memorial University's AZFP mounted on a glider and visualize the water column in Trinity Bay. In this field experiment, we produce results that explore the attenuation of sound in seawater at specific frequencies, discuss whether a repeated acoustic signal is logically the bottom or a pycnocline, and talk about the practicalities of visualizing large bodies of water with the AZFP on a glider.

# 1 Introduction

The Acoustic Zooplankton Fish Profiler (AZFP) is a multi-frequency echosounder that is used to detect marine species of various sizes (Sheehan, 2021). Its original purpose was to be attached to a stationary structure such as a mooring, but in modern day, the AZFP is being used to augment traditional vessel-based sampling by being attached to gliders. Integrated into small autonomous underwater vehicles (AUVs) such as gliders, AZFPs can collect data at greater depths, closer to the coast-line, and over longer time periods than vessel-based sampling. These special scientific echosounders can hold up to four frequency channels, and possess the capability to study biomass, distribution, and behavior of zooplankton and fish by measuring acoustic back-scatter. Effective frequencies are correlated to specific organisms based on their size and associated back-scatter. Higher frequencies are optimal for detecting smaller creatures such as krill. The AZFP operates with very low power consumption making it ideal for long-term glider deployments. The purpose of this study was to test Memorial University's AZFP mounted on a glider and visualize the water column in Trinity Bay.

## 1.1 Echosounder Operation when Attached to a Glider

The principles of how an echosounder functions will be important to understand throughout this paper. A transmitter produces a burst of electrical energy at a particular frequency. The transmitter output is applied to a transducer which converts the electrical energy into acoustic energy that propagates through the water in a directional beam. The width of the beam is inversely proportional to the specified frequency (Simmonds & MacLennan, 2005). As the acoustic pulse propagates through the water, it may encounter several targets along its path, like fish-schools or the seabed. Targets reflect the pulse, producing acoustic back-scatter (an echo) and some energy returns to the transducer. The transducer converts the echo back into electrical energy; a signal that can be visualized (see **figure 1**).

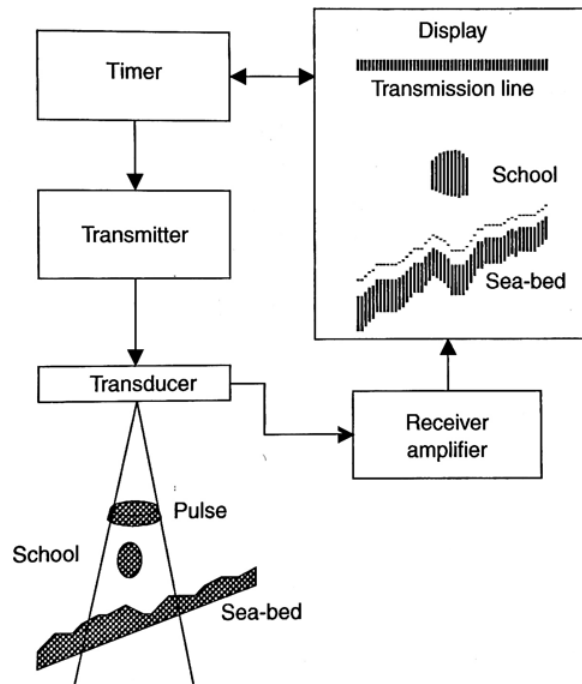


Figure 1: Concept of echosounding from page 71 of (Simmonds & MacLennan, 2005). The transmitted pulse generates echos from a fish school and the sea-floor.

Gliders are autonomous underwater vehicles (AUVs) of approximately 2 m in length that are capable of long-term deployments on the scale of months. Gliders move vertically by changing buoyancy. Buoyancy change is accomplished by moving hydraulic oil from a reservoir inside a pressure hull to inflate or deflate a rubber bladder external to the pressure hull (“Seaglider Pilot’s Guide”, 2021). The glider’s wings convert the vertical force provided by the variable buoyancy device into forward motion. They are able to travel in up-casts and down-casts on straight, diagonal lines. The AZFP is mounted on the bottom of the glider used in this field study and is set up to send beams downwards into the water column. In this configuration, only back-scatter data collected on down-casts is usable.

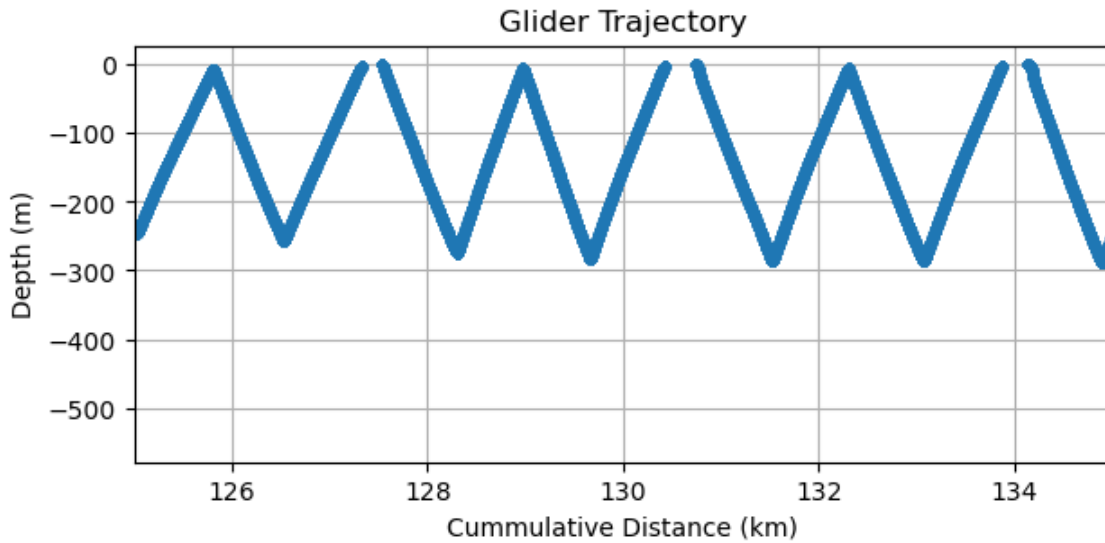


Figure 2: The glider is constrained to travel in up-casts and down-casts on straight, diagonal lines. In this configuration, only back-scatter data collected on down-casts is usable. There are disconnects at the surface because the glider does not collect data there.

## 1.2 Glider Deployment and Sensors

A G3 Slocum Glider from Teledyne Webb Research codenamed "Barnacle" was deployed from Heart's Content, Newfoundland on November 20th, 2022 with the aid of a fishing boat. The whole deployment lasted ten days (see **figure 3** below). "Barnacle" was equipped with Conductivity, Temperature, Depth probes (CTD), and an AZFP. Conductivity can be measured by applying a voltage between two electrodes immersed in the sea-water. The drop in voltage caused by the resistance of the water is used to measure conductivity (thus salinity). The salinity, pressure, and temperature records from the CTD provide necessary parameters to accurately calibrate the volume back-scatter coefficient to visualize the acoustic data.

## 1.3 Water Properties of Trinity Bay

Trinity Bay is an inlet located off of eastern Newfoundland with a maximum depth of 600 m. The cold waters of the Labrador Current in unison with river run-off from the western

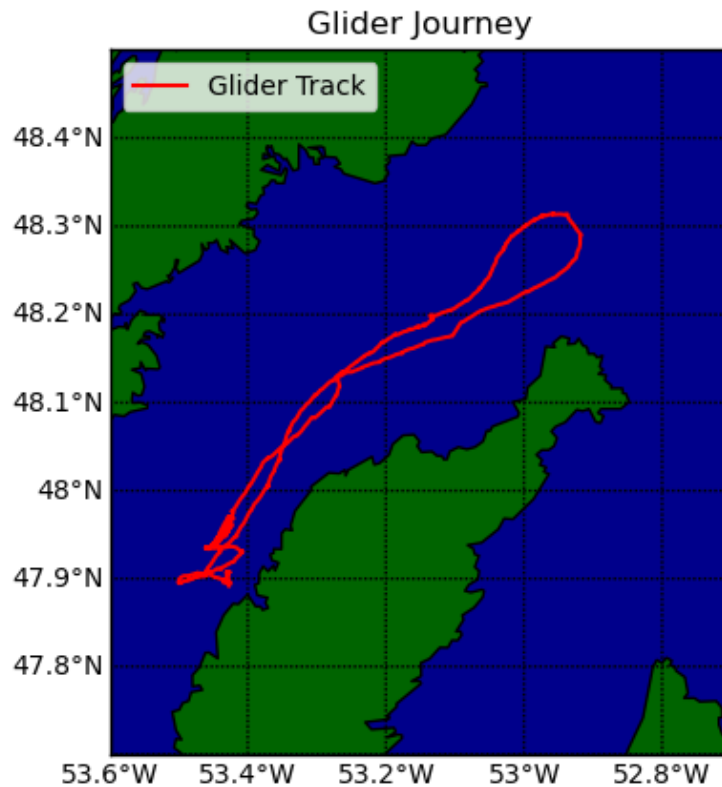


Figure 3: "Barnacle's" Journey in Trinity Bay, November 20th to 30th. Throughout these 10 days, the glider collected 1 054 001 elements with the CTD probes and collected a couple hundred AZFP profiles.

side of the Bay cause stable-stratification with fresh water on the surface and cold, highly oxygenated water at depth. Trinity Bay's thermocline is characterized by a temperature change of over  $14^{\circ}\text{C}$  between the surface and 75 m, and a cold intermediate layer (70-200 m) of approximately  $-1^{\circ}\text{C}$ . The remainder of the depth demonstrates temperatures of just below  $1^{\circ}\text{C}$  (von Oppeln-Bronkowski & de Young, 2021).

## 2 Theoretical Background

Some relevant background in Acoustical Oceanography is essential to our understanding of the results produced from this field experiment. The AZFP works by using echolocation, meaning that a suitable signal level from scattered sound is necessary. In addition to geometrical spherical spreading losses, sound in water is attenuated by various terms that are frequency dependent. Relevant equations presented in sections 2.1, 2.2, and 2.3 are taken from Medwin and Clay, 1998. For section 2.4 about the Volume Back-scatter coefficient, presented material can be found from Simmonds and MacLennan, 2005.

### 2.1 Newton's Second Law for Acoustics

How deep into the water channel is the AZFP able to collect acoustic back-scatter? To begin understanding attenuation of sound waves due to absorption losses in seawater, we begin with **Newton's Second Law for Acoustics** in one dimension.

First, imagine that a disturbance in the seawater is caused by a sudden expansion from a small spherical source. The local pressure and density increases because the surrounding water does not instantaneously move to allow space for the expansion. If we consider a region far away from the source and assume plane wave propagation, the variations of pressure (and density) of a fluid particle are functions of the direction of propagation.

For discussing acoustic forces in this paper, we refer to the incremental acoustic pressure as simply  $p$ , and the unchanging ambient pressure of the seawater as  $p_a$ . Similarly, ambient density  $\rho_a$  is the density of seawater, and  $\rho$  is the acoustic density. The ambient pressure and density are much greater than the acoustic pressure and density. See **figure 4** for a better understanding of the effects acoustic pressure and density have on a fluid particle.

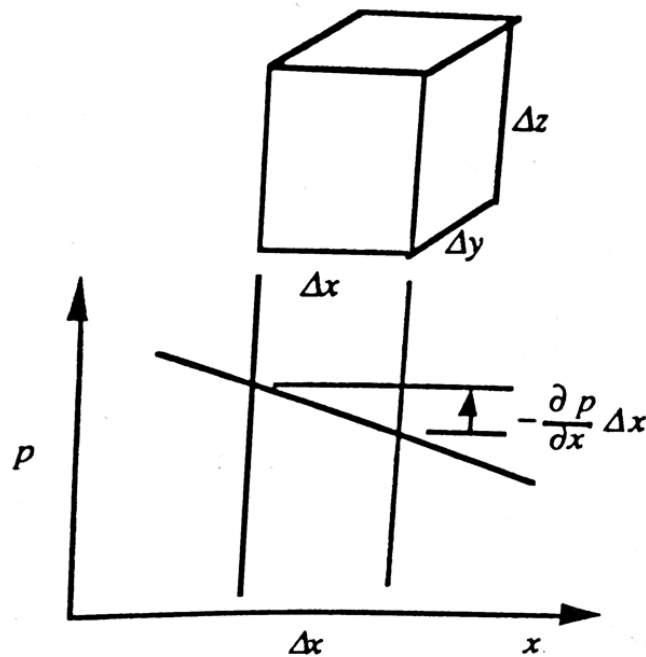


Figure 4: Acoustic pressure differential across a small volume of fluid from page 36 of (Medwin & Clay, 1998). The pressure differential causes the mass  $\Delta x \Delta y \Delta z \rho_a$  to move to the right.

The total pressure and density are sums of the ambient and acoustic contributions:

$$p_T = p_a + p$$

$$\rho_T = \rho_a + \rho$$

The net pressure in the positive  $x$  direction acting on a water particle is

$$p = -\frac{\partial p}{\partial x} \Delta x \tag{1}$$

Take velocity of fluid particles as a three dimensional vector in Cartesian coordinates  $\vec{u} = (u, v, w)$ , note that the mass of a water particle is  $\rho_a \Delta x \Delta y \Delta z$ , and keep in mind that pressure is simply force per unit area. Newton's law  $F = ma$  therefore yields

$$-\frac{\partial p}{\partial x} \Delta x \Delta y \Delta z = \rho_a \frac{\partial u}{\partial t} \Delta x \Delta y \Delta z \quad (2)$$

which simplifies to

$$-\frac{\partial p}{\partial x} = \rho_a \frac{\partial u}{\partial t} \quad (3)$$

Each component can be generalized as follows

$$\begin{aligned} -\mathbf{i} \frac{\partial p}{\partial x} &= \mathbf{i} \rho_a \frac{du}{dx} \\ -\mathbf{j} \frac{\partial p}{\partial y} &= \mathbf{j} \rho_a \frac{dv}{dy} \\ -\mathbf{k} \frac{\partial p}{\partial z} &= \mathbf{k} \rho_a \frac{dw}{dz} \end{aligned}$$

$\vec{u}$  is a function of space and time and thus must be differentiated implicitly. For the  $x$  component this looks like

$$\frac{du}{dt} = \frac{\partial u}{\partial t} + \frac{\partial u}{\partial x} \frac{\partial x}{\partial t} = \frac{\partial u}{\partial t} + u \frac{\partial u}{\partial x} \quad (4)$$

Where  $\frac{\partial u}{\partial t}$  is the local acceleration of the fluid particle and  $u \frac{\partial u}{\partial x}$  is the convective acceleration. For a plane wave propagating in the  $x$  direction,  $u = u(t - x/c)$ . Noting that  $c$  denotes the speed of sound, we find that

$$u \frac{\partial u}{\partial x} = -\frac{u}{c} \frac{\partial u}{\partial t} \quad (5)$$

In linear acoustics it is required that  $u/c \ll 1$ , so we can drop the convective acceleration term and write  $\frac{du}{dt} = \frac{\partial u}{\partial t}$ . Generalizing equation 3 to three dimensions, we can write

$$\nabla p = -\rho_a \frac{\partial \vec{u}}{\partial t} \quad (6)$$

This is an Euler Equation that will allow us to discuss attenuation and absorption loss, which will help us understand how far into a column of seawater the AZFP can visualize acoustic back-scatter.

## 2.2 Attenuation and Viscosity

The exponential attenuation of plane waves in acoustics happens when energy is lost to heat or chemical absorption. A plane wave loses acoustic pressure proportional to the original pressure  $p$  and distance it travels. In other words

$$\begin{aligned} dp &= -\alpha_e p dx \\ p &= p_0 e^{-\alpha_e x} \end{aligned}$$

The amplitude decay coefficient  $\alpha_e$  has units of nepers/unit distance. A neper refers to a logarithmic unit for ratios such as gain or loss of electronic signals. It is often more desirable to use the common engineering unit of decibels, in which the amplitude decay coefficient is  $\alpha = \frac{1}{x} 20 \log_{10} \frac{p_0}{p} = 8.868 \alpha_e$ .

In developing our understanding of attenuation due to absorption loss in seawater, turn your attention to equation 6 presented in section 2.1. The complete acoustic force equation includes viscosities (Medwin and Clay, 1998):

$$\rho_a \frac{\partial \vec{u}}{\partial t} = -\nabla p + \left( \frac{4\mu}{3} + \mu_b \right) \nabla \nabla \cdot \vec{u} - \mu \nabla \times (\nabla \times \vec{u}) \quad (7)$$

where  $\mu$  is the dynamic coefficient of shear viscosity, and  $\mu_b$  is the dynamic bulk vis-

cosity. The shear viscosity is the ratio of shearing stress compared to the rate of strain. Each component of the stress is due to a shearing force parallel to an area, caused by a velocity gradient perpendicular to the area. For example, the shearing force in the  $x$  direction is caused by a velocity gradient in the  $y$  direction:

$$\frac{F_x}{A} = \mu \frac{\partial u}{\partial y} \quad (8)$$

The bulk viscosity is important because we are discussing acoustic waves in water which are compressible. Some physical intuition behind  $\mu_b$  is that it only appears in the divergence term of equation 7, which is proportional to the rate of change in density because of acoustic conservation of mass. Consider a plane wave in the  $x$  direction, so that the cross product term in equation 7 disappears.

$$\rho_a \frac{\partial u}{\partial t} = -\frac{\partial p}{\partial x} + \left(\frac{4\mu}{3} + \mu_b\right) \frac{\partial^2 u}{\partial x^2} \quad (9)$$

We introduce acoustic conservation of mass and the plane-wave relation (the origins of the plane-wave relation will be discussed in section 2.3).

$$\rho_a (\nabla \cdot \vec{u}) = -\frac{\partial \rho}{\partial t} \quad (10)$$

$$p = \rho c^2 \quad (11)$$

Differentiating equation 9 with respect to  $x$  and using equations 10 and 11, we obtain the wave equation with additional viscosity terms from equation 7. Now we have an equation that describes the influence that viscosities have on a plane wave propagating through seawater.

$$\frac{\partial^2 \rho}{\partial x^2} + \frac{(\frac{4\mu}{3} + \mu_b)}{\rho_a c^2} \frac{\partial}{\partial t} \frac{\partial^2 p}{\partial x^2} = \frac{1}{c^2} \frac{\partial^2 p}{\partial t^2} \quad (12)$$

### 2.3 Molecular Relaxation

Recall the physical properties about  $\mu$  and  $\mu_b$  discussed in section 2.2. It takes a finite time for a fluid to relax back to its original state after a pressure disturbance. Chemical relaxation in seawater involves ionic dissociation (the breaking up of an ionic compound into its original constituents) that is activated and deactivated by pressure changes caused by sound increasing and decreasing in density. Magnesium sulfate and boric acid are the main contributors to sound absorption in seawater, even though they are much less abundant than the dominant ocean salinity constituents of sodium and potassium chloride.

Attenuation due to molecular relaxation in seawater is dependent on the plane-wave relation we used to derive equation 12. It comes from the acoustical version of Hooke's Law. In this case, the stress is considered to be acoustic pressure  $p$ , and the strain is considered to be the relative change in density  $\frac{\rho}{\rho_a}$ . The proportionality constant is the bulk modulus for elasticity  $E$ .

$$p = \left(\frac{E}{\rho_a}\right)\rho. \quad (13)$$

Taking the partial derivative with respect to  $x$  of equation 3 and the partial derivative with respect to  $t$  of the  $x$  component from the acoustical conservation of mass (equation 10) we obtain the following wave equation in one dimension:

$$\frac{\partial^2 p}{\partial x^2} = \left(\frac{\rho_a}{E}\right)\frac{\partial^2 p}{\partial t^2}$$
$$c^2 = \frac{E}{\rho_a}$$

The plane wave equation does not include any term that can respond to processes that absorb energy we add as the wave propagates. In order to include attenuation due to molecular

relaxation requires that a time dependent term be added to our simple version of Hooke's Law (equation 13). Adding a time dependent term gives:

$$p = c^2\rho + b\frac{d\rho}{dt} \quad (14)$$

where  $b$  is a scaling constant. Relaxation time  $\tau_r$  is found by setting acoustic pressure to 0 in equation 14 and then integrating to solve for  $\rho$ .

$$\rho = \rho_0 e^{-\frac{t}{\tau_r}}$$

$$\tau_r = \frac{b}{c^2}$$

The value of the relaxation time depends on the fraction of molecules active in the relaxation process. This means that it also depends on the temperature and pressure of the liquid.

We just derived the wave equation while discussing the acoustic version of Hooke's Law at the beginning of this section. We can go through the exact same process but instead of using equation 13 after eliminating the common second derivative, use equation 14. In terms of acoustic density we have

$$\frac{\partial^2 \rho}{\partial x^2} + \tau_r \frac{\partial}{\partial t} \frac{\partial^2 \rho}{\partial x^2} = \frac{1}{c^2} \frac{\partial^2 \rho}{\partial t^2} \quad (15)$$

with proposed solution

$$\rho = \rho_0 e^{i(\omega t) - (ik_r + \alpha_e)x} \quad (16)$$

Where  $k_r$  is the propagation constant and  $\alpha_e$  is the absorption coefficient that was introduced in section 2.2. Plugging equation 16 into equation 15 and equating the reals and

imaginaries gives two equations which you can solve simultaneously to find the exponential attenuation rate and the real propagation constant, the dispersive phase speed  $c_r$ .

$$\alpha_e = \frac{\omega^2 \tau_r c_r}{2c^2(1 + \omega^2 \tau_r^2)} \quad (17)$$

Because of relaxation effects in seawater,  $c \approx c_r$ . Define relaxation frequency as

$$f_r = \frac{1}{2\pi \tau_r} \quad (18)$$

We can now rewrite attenuation rate in nepers/distance and decibels/distance.

$$\begin{aligned} \alpha_e &= \frac{\frac{\pi f_r}{c} f^2}{f_r^2 + f^2} \\ \alpha &= \frac{A f_r f^2}{f_r^2 + f^2} \\ A &= \frac{8.68\pi}{c} \end{aligned}$$

It is useful to analyze attenuation per wavelength, because it is then easy to observe that attenuation approaches zero for very high and very low frequencies.

$$\alpha \lambda = (A c f_r) \frac{f}{f_r^2 + f^2} \quad (19)$$

For large  $f$ ,  $f_r^2 + f^2 \approx f^2$ . This means that  $\alpha \lambda$  approaches  $\frac{1}{f}$  and goes to 0 for high frequency. Physically what happens is the relaxing molecules do not respond fast enough to dissociate. When  $f$  is very small,  $f_r^2 + f^2 \approx f_r^2$ , so  $\alpha \lambda \approx \frac{f}{f_r^2}$ . For low frequency, molecular relaxation happens in step with the sound wave. When the frequency of the sound wave is approximately the same as relaxation frequency, the activated molecules will release energy from a condensation into a rarefaction. In the latter circumstance, some of the energy from the sound wave is dissipated into the water as heat.

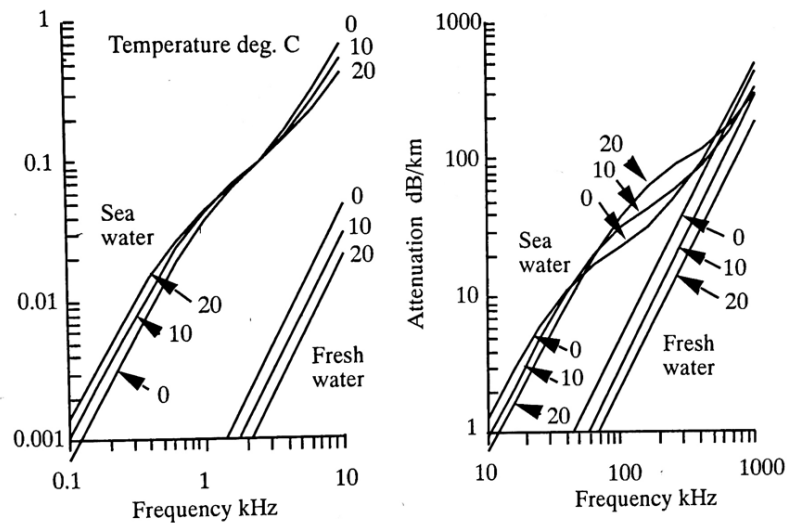


Figure 5: Sound pressure attenuation rate in dB/km in fresh and seawater from page 109 of (Medwin & Clay, 1998). Calculated from Francios and Garrison (1982). Parameters at pH=8; S=35ppt; and depth  $z=0$  m.

Figure 5 (Medwin & Clay, 1998) shows that attenuation as a function of frequency for seawater is notably greater than attenuation in freshwater, because freshwater is only affected by the viscous attenuation terms. The two steps seen in the figure at about 2 kHz and 300 kHz correspond to the relaxation times of Boric acid and Magnesium Sulfate respectively. At frequencies above 500 kHz, attenuation in seawater and freshwater begin to overlap.

## 2.4 Volume Back-scatter Coefficient and Target Strength

The last section of background theory required to analyze the figures in the results of this paper is the idea behind target strength and volume back-scatter coefficient  $s_v$ .

The target strength of back-scatter from an object is a logarithmic measurement of the proportion of incident energy that is back-scattered by the target. Back-scattering cross section  $\sigma_{bs}$  is measured in units of area and defined in terms of the intensities of the incident ( $I_i$ ) and back-scattered ( $I_{bs}$ ) waves.

$$\sigma_{bs} = R^2 I_{bs} / I_i \quad (20)$$

$R$  refers to the distance from the target at which intensity is measured.  $R$  must be large enough to be outside of the near-field of the target but not so large that absorption losses become significant.

When individual targets are very small and there are multiple of them in a sampled volume, their echos combine to form a continuous signal with varying amplitude. Individual targets cannot be resolved, but echo intensity will be a measurement of the biomass in the water column (Simmonds & MacLennan, 2005).

To formally understand the basic measurement of ocean acoustics  $s_v$  we turn to echo-integration. The echo-integrator is an echosounder with output connected to a device which accumulates the energy from the recieved signal. Take  $v(t)$  as the voltage produced by the echosounder at time  $t$ . The echo-integrator output due to a singular transmission is therefore

$$E_i = \int_{t_1}^{t_2} |v(t)|^2 dt \quad (21)$$

$E_i$  is called the echo-integral. The echo-integrator collects many echo-integrals from many transmissions, and fish density can be calculated from the mean echo-integral.

The volume back-scattering coefficient is obtained from the echo-integral, and is formally defined as a sum of all the discrete targets contributing to echos from the sampled volume  $V_o$ .

$$s_v = \sum \frac{\sigma_{bs}}{V_o} \quad (22)$$

The logarithmic equivalent of volume scattering-coefficient is the volume back-scattering strength  $S_v$  measured in decibels.

### 3 Processing

The glider has two independent instruments, the CTD and AZFP. Data from the two instruments is lined up using timestamps from the respective data files. The AZFP only collects correctly orientated data when the echosounder is pointing straight down. Since the AZFP is mounted on the bottom of the glider at an angle of about  $22.5^\circ$ , the pitch of the down-casts should not be less than  $-30^\circ$  or greater than  $-15^\circ$  (Sheehan, 2021) in order for the data to be usable. The data was sorted into down-casts (good data) and up-casts (bad data) by sorting through the gliders record of tilt (see **figure 6**).

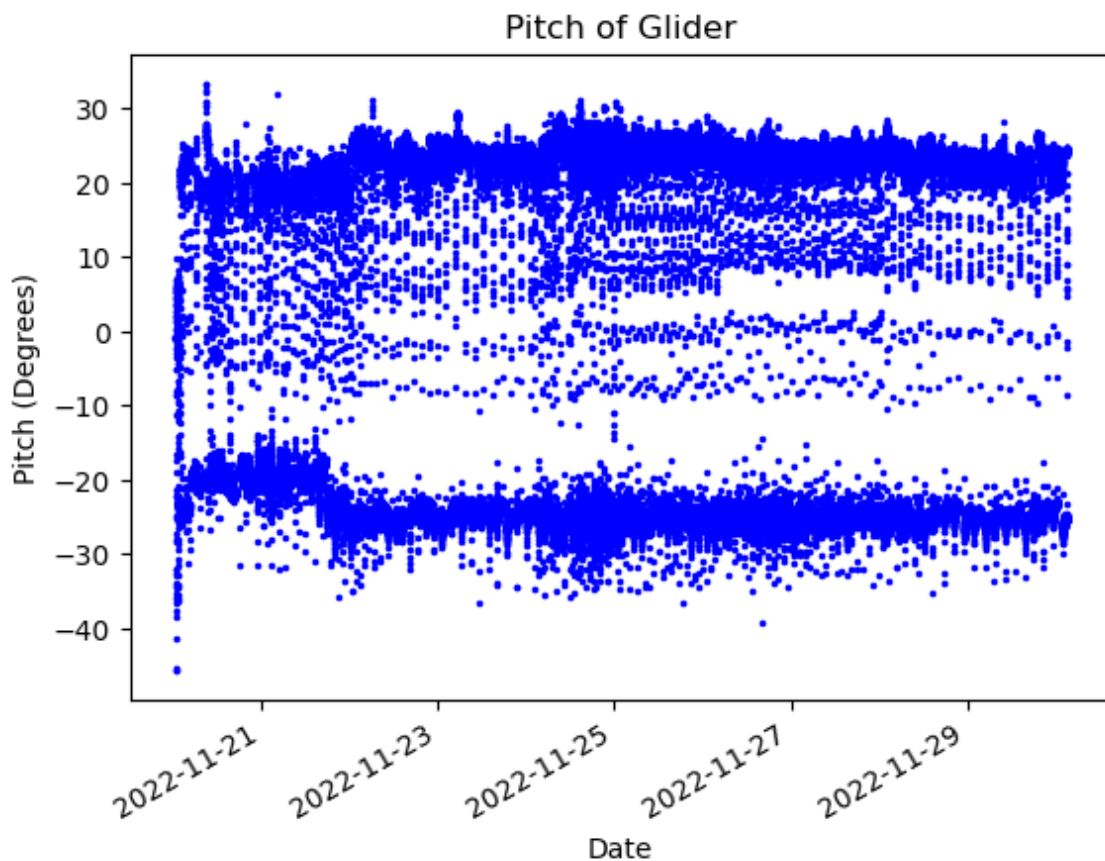


Figure 6: Pitch of the glider throughout the entire deployment.

The average salinity, temperature, and pressure (S,T,P) values from the glider cast are

given as parameters into Echotype (*Data Processing*, 2022) in order to account for exponential attenuation and calculate the volume back-scatter coefficient  $S_v$ . Echotype converts raw AZFP files indicated by the extension '.01A' into standard netcdf files, which are widely used in oceanographic research and are supported by a range of Python packages, specifically 'xarray' instead of the more popular data organizer 'pandas'. This requires a calibration file (.XML) for the sensor in addition to the .01A data file (Sheehan, 2021).

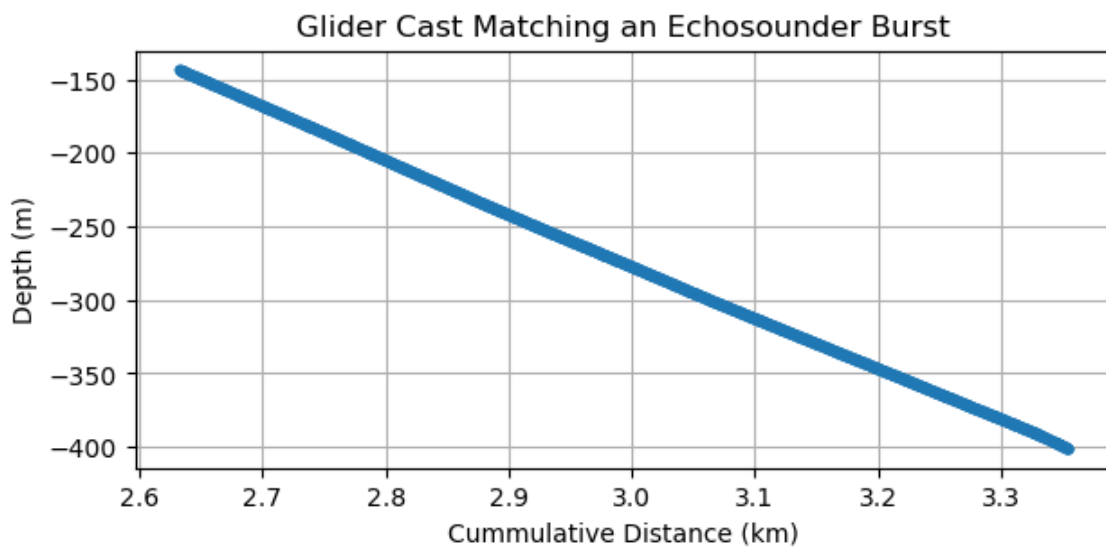


Figure 7: A down-cast associated with an AZFP echo-burst in terms of cumulative distance of the deployment. The average (S,T,P) values from this down-cast are input into Echotype to account for exponential attenuation of the sound-wave during processing.

The transducer used to convert electrical energy into acoustic energy through the water is a resonant system. When you transmit a pulse into the seawater, the transducer resonates with the voltages associated with the transmit signal, making any data collected during this time invalid. In order to avoid the corrupted data, the first 100 elements of the  $S_v$  array are replaced with zeros.

Network Common Data Form (netcdf) is a hierarchical data format used predominantly in oceanographic research and climate science. Netcdf is self describing, meaning that all of the metadata needed to work with the data can be contained within the netcdf file itself. The

logical organization of the netcdf files is shown in **figure 8**.

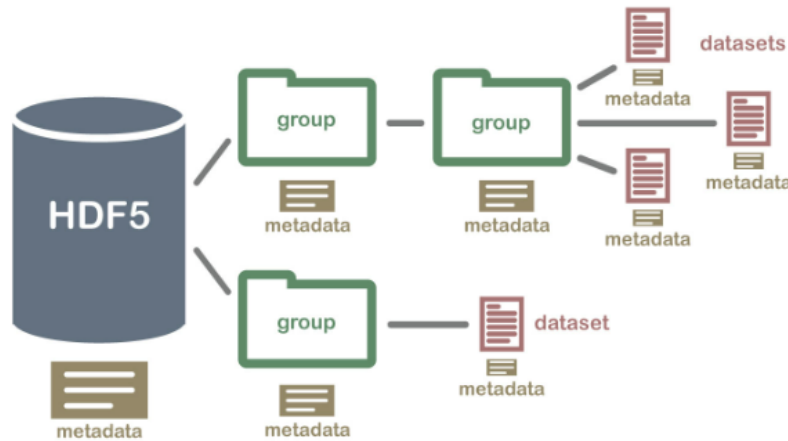


Figure 8: Diagram of netcdf file format from (*Lesson 1. Introduction to the NetCDF4 Hierarchical Data Format, 2020*) showing that all metadata required to work with the data is in a hierarchical flow.

The convenience of working with the hierarchical format of netcdf while processing the acoustic data revealed an important flaw within the AZFP apparatus itself for this particular deployment. The back-scatter from the four frequency channels of the AZFP (67 kHz, 120 kHz, 200 kHz, and 455 kHz) are nested within the sub-group 'Beam\_group1' that is inside the group 'sonar'. Data plots initially reported echos reaching farther for higher frequency channels than for the lower frequency channels, inconsistent with their expected sonar performance. Direct inspection of the nested data from the netcdf files revealed that the apparatus was not storing the back-scatter collection to the correct frequency channels. That is, The 67 kHz echos were being stored to the 455 kHz designated file storage, the 120 kHz echos to the 200 kHz file storage, the 200 kHz echos to the 120 kHz file storage, and the 455 kHz echos to the 67 kHz file storage. This error not only affects the way we must label our acoustic diagrams, but also has caused corruption in processing the volume-backscatter coefficient. The smoothness of the  $S_v$  color profile is not what is expected of typical echo-data, leading to the conclusion that there is an error running the data through Echopype for calibration due to the apparatus flaw.

## 4 Results

### 4.1 Back-scatter Diagrams with Different Frequencies

The effects of molecular relaxation and the different attenuation of the sound waves at specific frequencies (see sections 2.2 and 2.3) are very apparent by viewing **figures 9,10,11 and 12**. All of these figures are the same down-cast but are associated with different frequencies. The color-bar is the back-scatter amplitude  $S_v$ , discussed in section 2.4. The signal shown between 400 m and 450 m could either be the bottom or a pycnocline (sudden change in water density with depth). We will analyze the thermocline and the salinity profile collected with the CTD probes in the next section to show why that signal is most likely the sea-floor. The 455 kHz channel demonstrates an echo-range of about 50 m, the 200 kHz channel about 100 m, 120 kHz about 150 m, and 67 kHz also about 150 m.

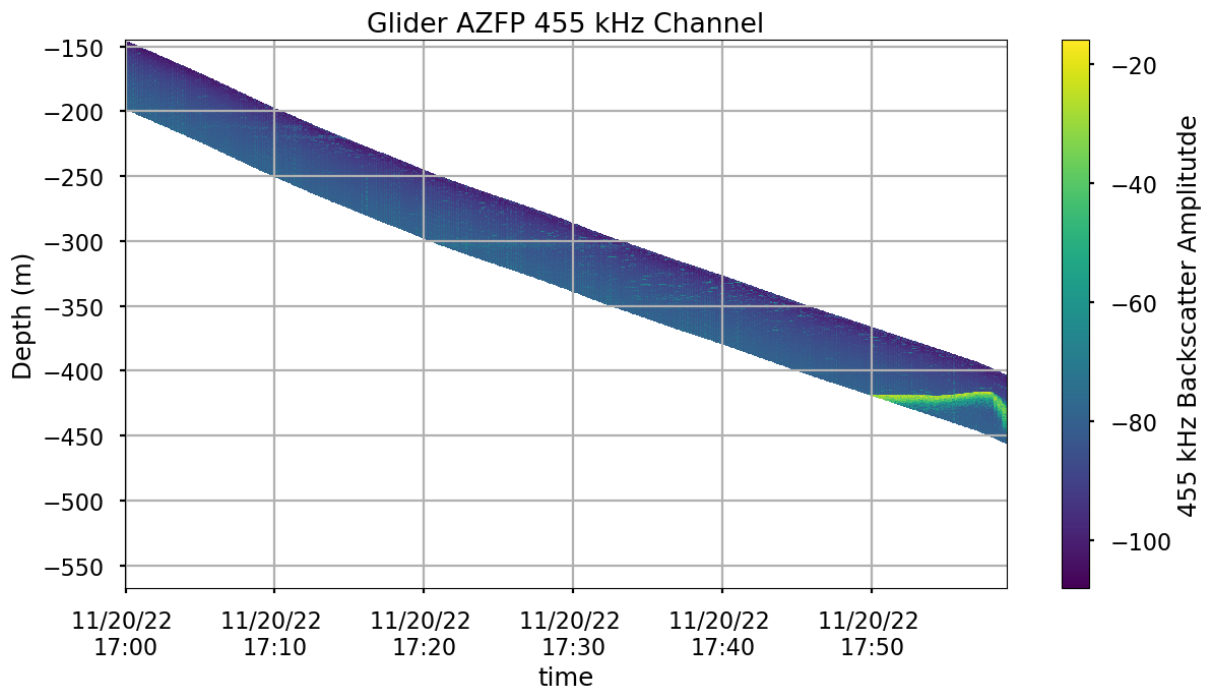


Figure 9: Echo diagram of a down-cast, 455 kHz

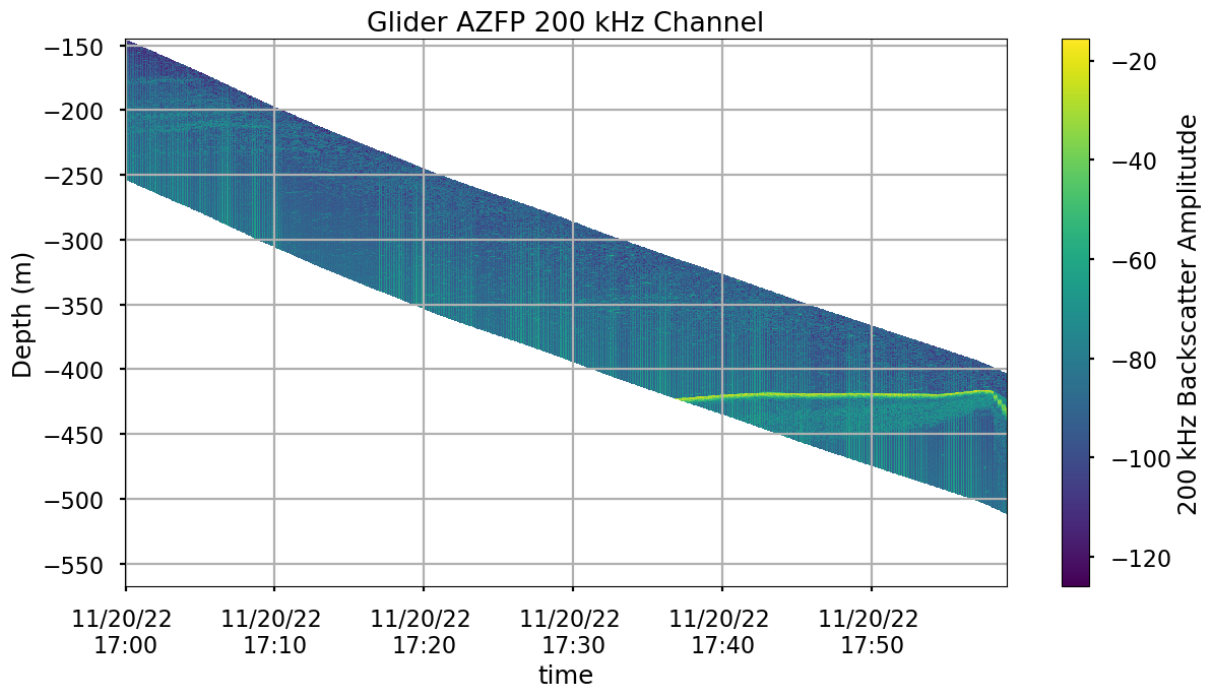


Figure 10: Echo diagram of a down-cast, 200 kHz

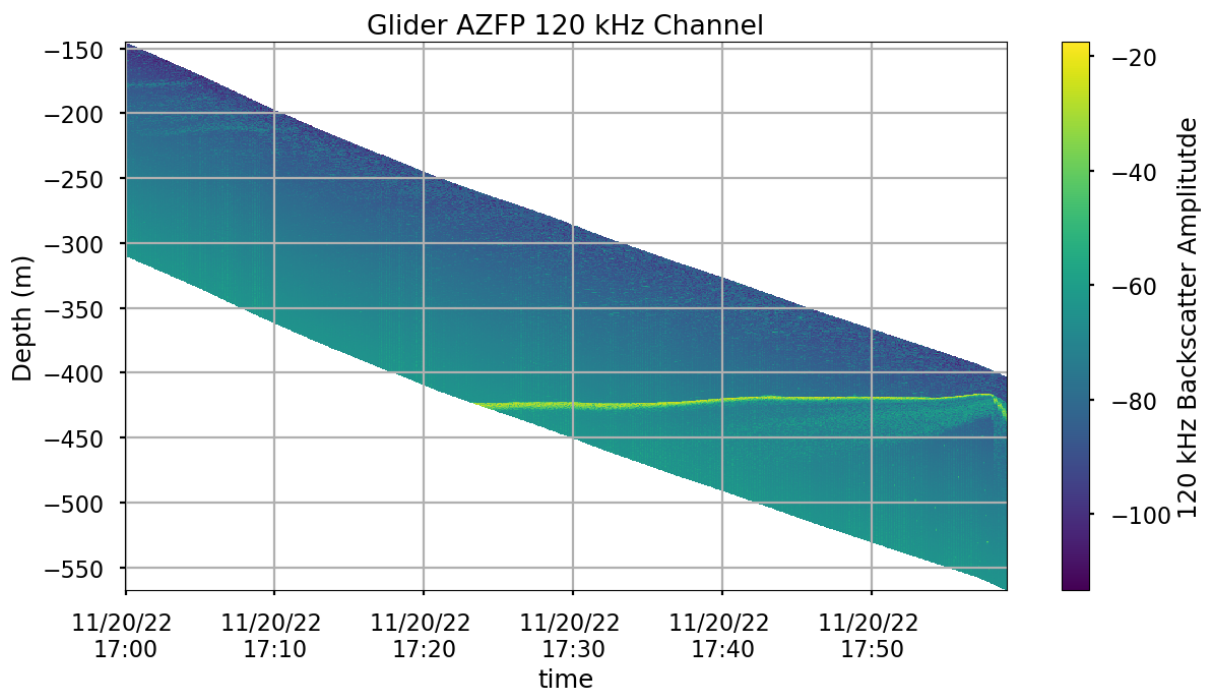


Figure 11: Echo diagram of a down-cast, 120 kHz

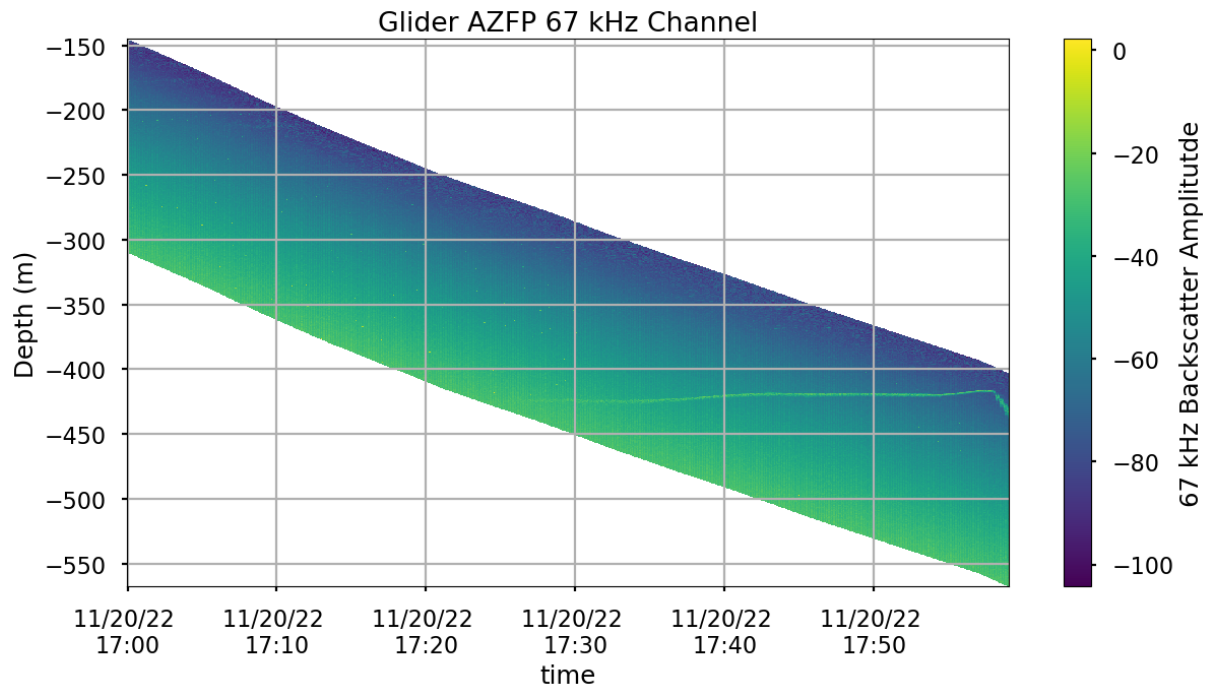


Figure 12: Echo diagram of a down-cast, 67 kHz

## 4.2 Merging Multiple Glider Casts

One of the primary goals of this field experiment is to understand what issues may arise while trying to use the AZFP on a glider to visualize Trinity Bay (or any large body of water for that matter). Below are AZFP profiles stitched together in attempt to visualize the Bay over a greater period of time.

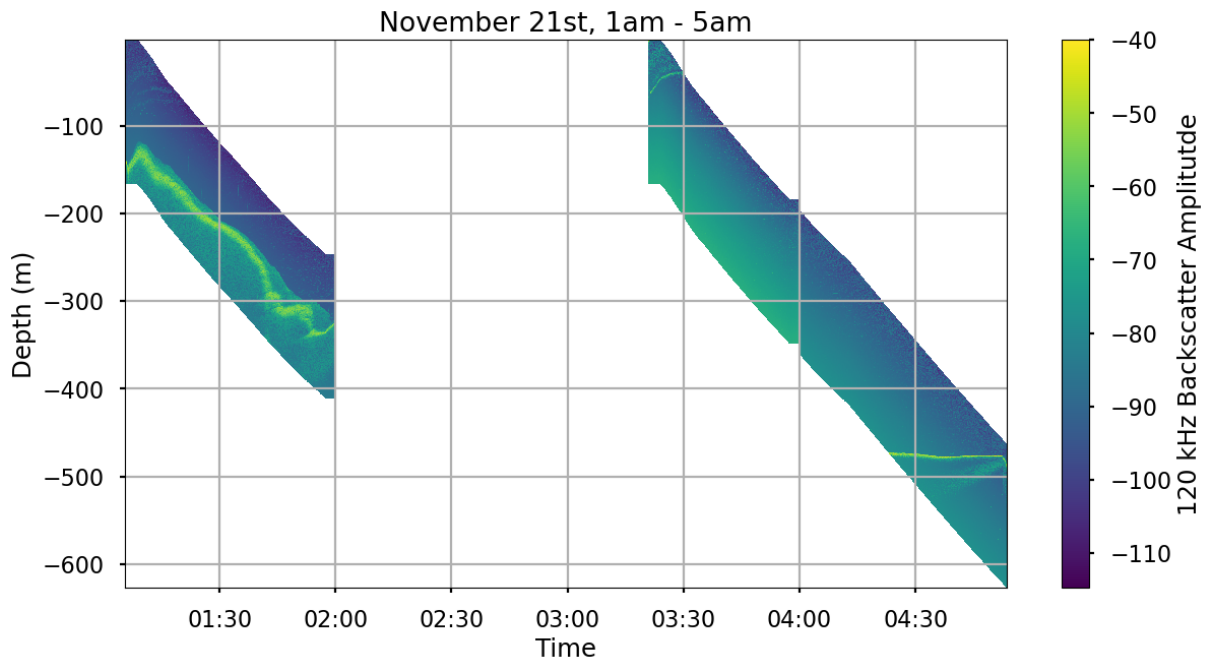


Figure 13: Three AZFP collections stitched together. Frequency channel is 120 kHz. The subtle disconnect on the second down-cast is the beginning of a new AZFP collection.

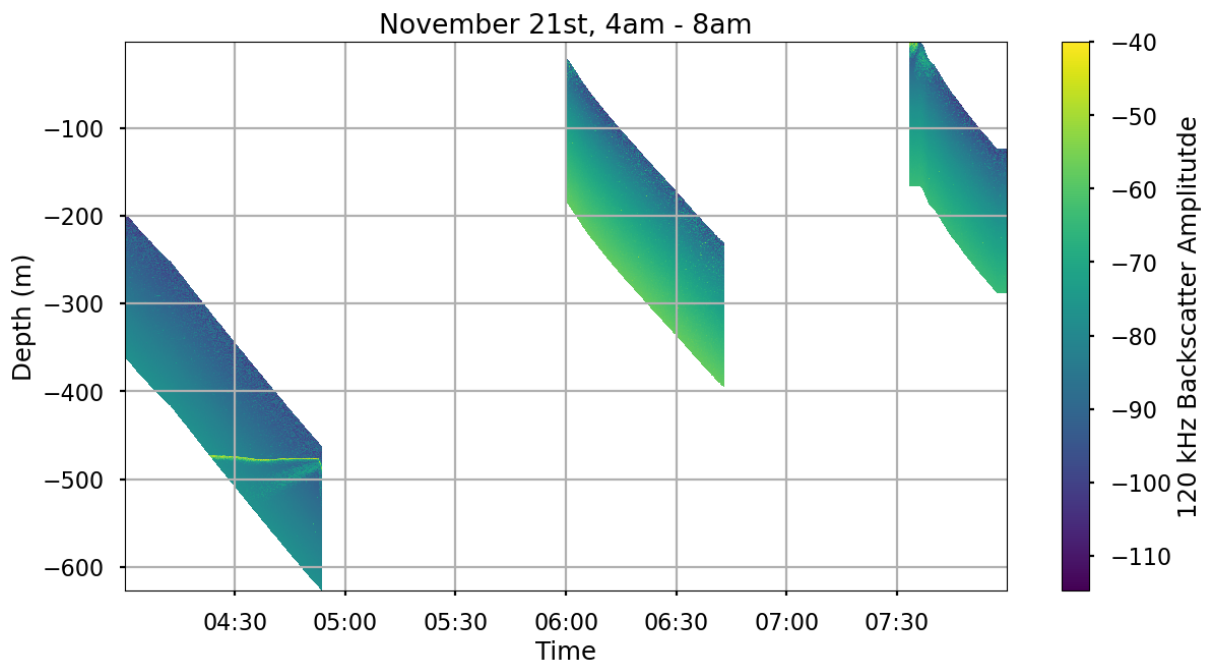


Figure 14: A combination of three AZFP collections stitched together. The frequency channel was 120 kHz. The Ultimate goal is to visualize a large portion of Trinity Bay.

In **figure 13**, we observe the difficulty of having the AZFP orientated to only collect usable echos when the glider is within the pitch range  $-30^\circ$  to  $-15^\circ$ . The back-scatter collected at 3:30 am follows the gliders motion as it is transitioning from an up-cast into a down-cast. Due to the fact that that the AZFP is mounted at about a  $22.5^\circ$  angle on the bottom of the glider, this data is unusable and indicates a need to mask out any pitch data out of the range  $-30^\circ$  to  $-15^\circ$ . Since we use average (S,T,P) values per glider cast, the calibration values between 3:30-4:00 am and 4:00-5:00 am are not the same because they are separate casts. Something even more notable is that the glider cast from 3:30 to 4:00 am ends prematurely because of a wrinkle in the pitch data record, resulting in the processing software chopping the file and starting a new down-cast.

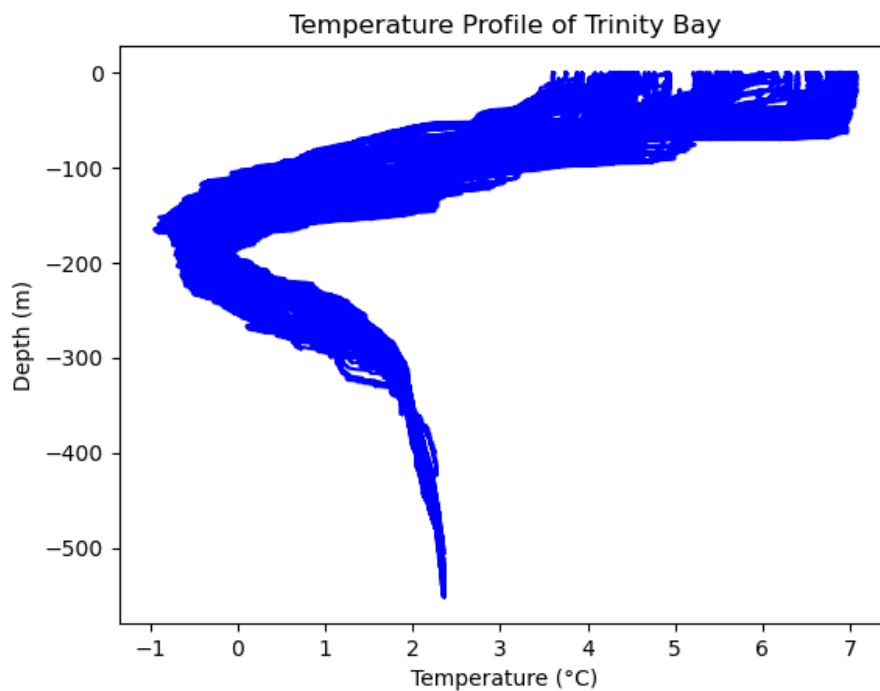


Figure 15: The Temperature Profile of Trinity Bay generated from the raw data of the CTD probes from the entire deployment.

The wrinkle in the pitch data occurs around 200 m depth (according to **figure 13**). Judging from the temperature profile (**figure 15**), there is a sudden change in density gradient at about 200 m. It is likely that the glider is responding to the shift in density gradient by varying

pitch in an unexpected way.

### 4.3 Interpreting Repeated Acoustic Signal

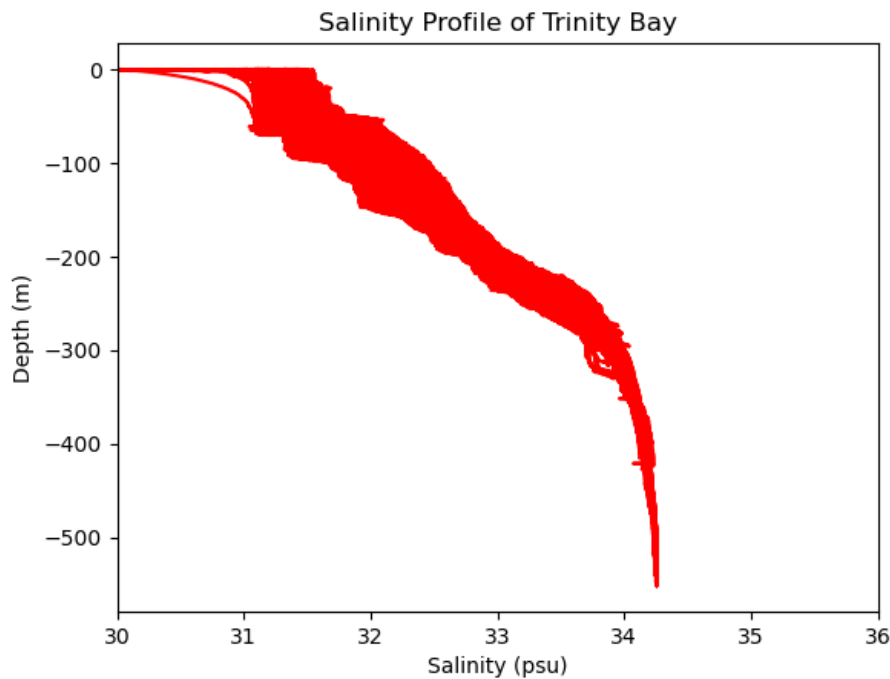


Figure 16: The Salinity profile of Trinity Bay generated from the from the CTD data of the entire deployment.

Something notable from **figures 9-14** is that there is a similar acoustic signal at different times when the glider dives near the maximum depth of Trinity Bay. If this signal does not represent the bottom, the only other option is that it is representing a pycnocline. Observe the temperature and salinity profiles **figures 15 and 16** where the repeated acoustic signal is showing up between 400 m and 450 m. At the relevant depths the temperature is consistently between 2°C and 3°C, and the salinity is consistently just above 34 psu. Therefore, the density is fairly consistent in this layer of water, with no reason to assume there is a pycnocline. Based on the latter statement, it is most likely that the repeated signal in our echo diagrams is from the sea-floor.

## 5 Discussion and Summary

Since we are able to process one AZFP profile, it is possible to visualize all down-casts and their associated echo diagrams onto a time-series. In testing the AZFP with this particular field experiment, it quickly became apparent that the AZFP was not synchronized to correctly capture acoustic data exclusively on down-casts (which is what it is set up for), so accurate visualization of the Bay using back-scatter is erratic. In (Sheehan, 2021), the method of sorting out correctly oriented glider-casts to plot useful AZFP data is to mask out any glider data that was not within the pitch range  $-30^\circ$  to  $-15^\circ$ .

Around depth of 200 m, the glider often experiences a wrinkle in the pitch data record, causing the processing software to cut the file off and initiate a new down-cast. When inspecting the temperature profile of the entire deployment, we see a dramatic shift in density at around 200 m. It is likely that the glider is responding to this shift in density gradient, causing the pitch to vary in an unexpected way.

Additionally, the smoothness of the  $S_v$  color profile is not what is expected of typical echo-data, leading to the conclusion that there is an error running the data through Echopype for calibration. This fault is caused by the frequency channels themselves being recorded into the raw AZFP files backwards; instead of 455 kHz, 200 kHz, 120 kHz, 67.5 kHz (the actual frequencies being recorded) they are labelled in the exact opposite order in the netcdf files. This means that we have to take this into consideration when labelling our acoustic diagrams, but also it is effecting the  $S_v$  output we are obtaining using Echopype.

A positive conclusion is that after addressing these issues in the apparatus, it is very possible to do a spatial temporal acoustic survey across a vast-body of water (like Trinity Bay) by using an AZFP mounted on a glider. It would be best used by teaming up with biologists that want to study specific animal behaviour, as the different frequency channels can be used to detect different organisms and calculate their biomass based on their acoustic back-scattering

strength.

## References

- Data Processing*. (2022). <https://echopype.readthedocs.io/en/stable/process.html>.
- Lesson 1. Introduction to the NetCDF4 Hierarchical Data Format*. (2020). <https://www.earthdatascience.org/courses/use-data-open-source-python/hierarchical-data-formats-hdf/intro-to-climate-data/>.
- Medwin, H., & Clay, C. S. (1998). *Fundamentals of acoustical oceanography*. Academic Press.
- Seaglider pilot's guide [Computer software manual]. (2021). School of Oceanography and Applied Physics Laboratory, University of Washington.
- Sheehan, A. (2021). Developing an open-source analysis pipeline for a glider-based acoustic zooplankton fish profiler (azfp).
- Simmonds, J., & MacLennan, D. (2005). *Fisheries acoustics theory and practice*. Blackwell Science.
- von Oppeln-Bronkowski, N., & de Young, B. (2021). Glider-based observations of  $CO_2$  in the labrador sea.